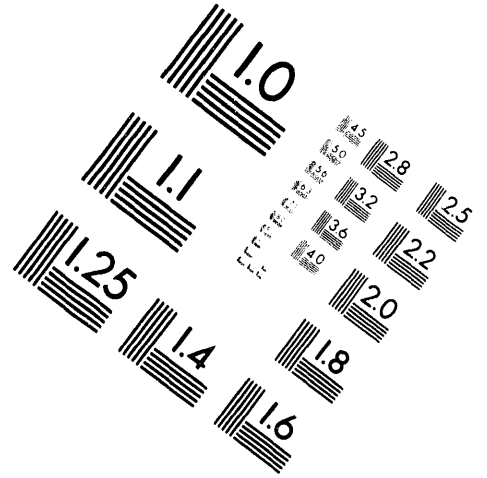
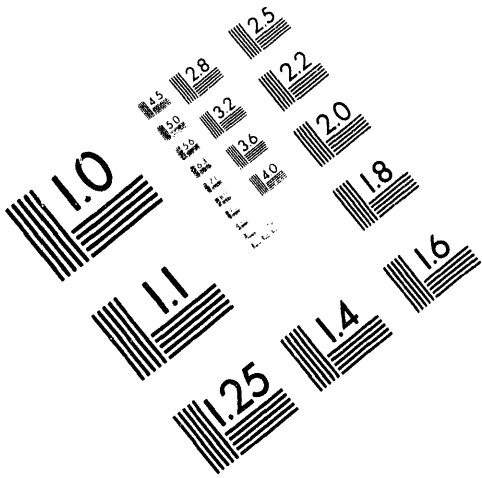




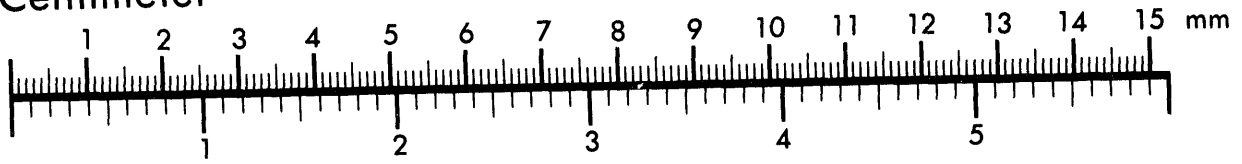
AIM

Association for Information and Image Management

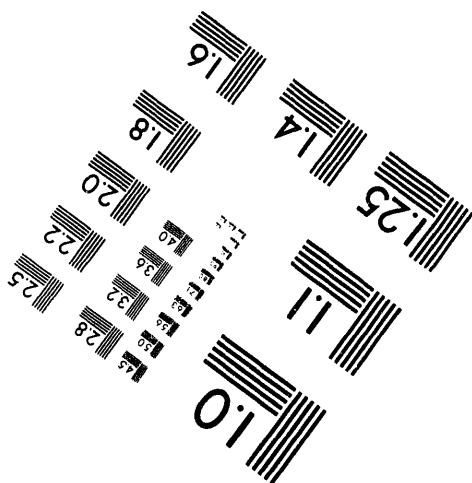
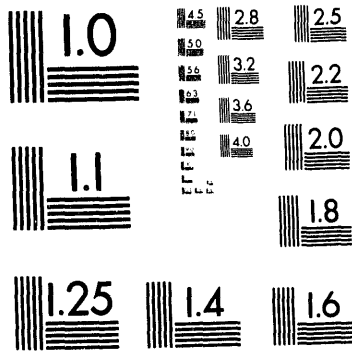
1100 Wayne Avenue, Suite 1100
Silver Spring, Maryland 20910
301/587-8202



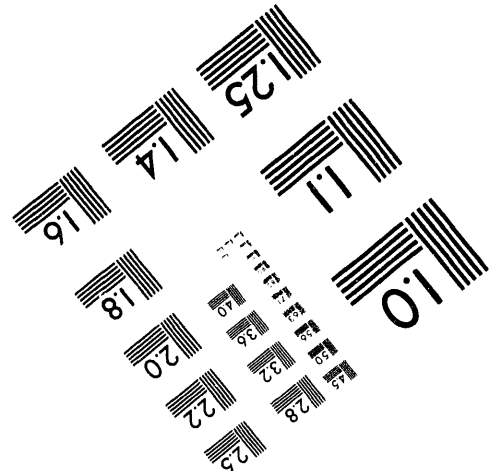
Centimeter



Inches



MANUFACTURED TO AIM STANDARDS
BY APPLIED IMAGE, INC.



1 of 1

Conf-940635--6

GA-A21756

**THE PARAMETRIC DEPENDENCE
OF THE SPATIAL STRUCTURE OF THE RADIAL
ELECTRIC FIELD AT THE PLASMA EDGE
IN THE DIII-D TOKAMAK**

by

**P. GOHIL, K.H. BURRELL, R.J. GROEBNER, J. KIM,
and R.P. SERAYDARIAN**

JULY 1994

DISTRIBUTION OF THIS DOCUMENT IS UNLIMITED



THE PARAMETRIC DEPENDENCE OF THE SPATIAL STRUCTURE OF THE RADIAL ELECTRIC FIELD AT THE PLASMA EDGE IN THE DIII-D TOKAMAK.

P. Gohil, K.H. Burrell, R.J. Groebner, J. Kim, and R.P. Seraydarian
General Atomics, P.O. Box 84508, San Diego, California 92186-9784

Much recent theoretical and experimental work has focused on the mechanisms controlling the transition from L-mode to H-mode and the subsequent improvement in transport and confinement.¹⁻¹³ Measurements of the radial electric field, E_r , with high spatial and time resolution at the L-H transition have led to an understanding of the improved confinement of the plasma edge in H-mode plasmas based on the stabilization of plasma turbulence by sheared $E \times B$ flow.¹⁻⁶ The radial electric field just inside the last closed flux surface (LCFS) changes dramatically at the L-H transition and a well-like structure in E_r forms simultaneously at the transition. At present, there is no accepted theory which gives the spatial structure of E_r near the plasma edge and which can predict its time evolution.

Present theories propose mechanisms for the generation of a negative E_r at the L-H transition, the bifurcation conditions for the transition and the stabilization of turbulence by sheared $E \times B$ flow.⁷⁻¹³ Although the various theories invoke different mechanisms to derive the negative E_r (e.g., ion orbit losses,^{8,13} Stringer spin-up,¹⁰ nonlinear transport theory,⁹ self-regulating turbulence^{11,12}), they have as yet to come into full agreement with the observed experimental results and, in particular, the observed behavior of the poloidal rotation and pressure gradient of the *main* ions at the transition.^{14,15} Furthermore, these theories need to be extended to explain the formation of the spatial structure of E_r at the transition and its temporal development into the H-mode. In order to help development of theories on the E_r profile, we have examined the dependence of the radial profile of E_r on different plasma parameters.

Experimental Conditions

The experimental investigations of the parametric dependence of the edge radial electric field were coordinated with investigations of the power threshold required for the H-mode transition. For each set of plasma parameters studied, a power scan with time was performed during each discharge. For cases where the H-mode power threshold was less than the injected power from an integral number of DIII-D neutral beams, one neutral beam was modulated at duty cycles of 25%, 50% and 75% of the full cycle period of 20 ms. This allowed for a more sensitive determination of the H-mode power threshold, but subsequently reduced the times at which data was available from the Charge Exchange Recombination (CER) spectroscopy diagnostic system.¹⁶ Typically, time points were available every 20 ms during the discharge. The full beam power was about 2.6 MW. The plasma conditions investigated covered the following range of plasma parameters in a lower single-null diverted configuration: plasma current, $I_p = 1.0-2.0$ MA; toroidal magnetic field, $B_T = 1.5-2.1$ T; ohmic target density, $\bar{n}_e = 2.0-4.0 \times 10^{19} \text{ m}^{-3}$; X-point height above the floor, $\Delta Z_x = 0-24$ cm; the plasma elongation, $\kappa = 1.8-2.0$; the gap between the LCFS at the z-location of the magnetic axis and the outside wall, $\text{gap}_{\text{out}} = 0-15$ cm; the gap between the inner LCFS at the z-location of the magnetic axis and the inner wall, $\text{gap}_{\text{in}} = 0-8$ cm. The following plasma parameters were investigated in a double-null diverted configuration: toroidal magnetic field, $B_T = 1.3-2.1$ T; plasma triangularity, $\delta = 0.7, 0.85$; inside gap, $\text{gap}_{\text{in}} = 1-8$ cm.

Measurements of the edge values of the ion temperature, T_i , the poloidal rotation, v_θ , and toroidal rotation, v_ϕ , in the DIII-D tokamak were made using a high resolution spectroscopy diagnostic system utilizing the active charge exchange recombination between the neutral atoms in the heating beams and impurity ions in the plasma. The C VI 5290.5 Å spectroscopic line was used for the measurements presented in this paper, whereby the ion temperature is determined from the widths of the Doppler broadened lineshape, the plasma rotation velocities, v_θ and v_ϕ , are determined from the Doppler shifted line centers and the relative impurity density is determined from the signal intensity of the line. The radial electric field, E_r , is calculated from the lowest order radial force balance equation for a single species, $E_r = (Z_I e n_I)^{-1} dP_I/dr - v_{\theta I} B_\phi + v_{\phi I} B_\theta$, where Z_I is the charge of the ion, n_I is the ion density, e is the electronic charge, P_I is the ion pressure, and B_ϕ and B_θ are the toroidal and poloidal magnetic fields, respectively. The CER system has the highest spatial resolution over a spatial extent of 4.6 cm at the outside plasma edge such that the spatial resolution of the flow velocities and E_r measurements is 0.6 cm and the spatial resolution of the T_i measurements is 0.3 cm. The minimum possible integration time for the measurements is 0.52 ms.

DISCLAIMER

This report was prepared as an account of work sponsored by an agency of the United States Government. Neither the United States Government nor any agency thereof, nor any of their employees, makes any warranty, express or implied, or assumes any legal liability or responsibility for the accuracy, completeness, or usefulness of any information, apparatus, produce, or process disclosed, or represents that its use would not infringe privately owned rights. Reference herein to any specific commercial product, process, or service by trade name, trademark, manufacturer, or otherwise, does not necessarily constitute or imply its endorsement, recommendation, or favoring by the United States Government or any agency thereof. The views and opinions of authors expressed herein do not necessarily state or reflect those of the United States Government or any agency thereof.

GA-A21756

**THE PARAMETRIC DEPENDENCE
OF THE SPATIAL STRUCTURE OF THE RADIAL
ELECTRIC FIELD AT THE PLASMA EDGE
IN THE DIII-D TOKAMAK**

by
**P. GOHIL, K.H. BURRELL, R.J. GROEBNER, J. KIM,
and R.P. SERAYDARIAN**

**This is a preprint of a paper to be presented at the
21st European Physical Society Conference on
Controlled Fusion and Plasma Physics, June 27-
July 1, 1994, Montpellier, France, and to be printed
in the *Proceedings*.**

**Work supported by
U.S. Department of Energy
Contract No. DE-AC03-89ER51114**

**GENERAL ATOMICS PROJECT 3466
JULY 1994**

MASTER

DISTRIBUTION OF THIS DOCUMENT IS UNLIMITED

 **GENERAL ATOMICS**

Parametric Dependence Of E_r

For all the plasma parameters investigated, both in single-null diverted and double-null diverted configurations, the general shape of the spatial profiles of the radial electric field was the same. This shape consisted of a negative well-like structure with the minimum of the E_r well located at or just inside the LCFS. The E_r values just inside the LCFS were negative for all the plasma parameters and conditions investigated, *with no exceptions*. The available data are too numerous to be represented adequately within the limited space of this paper and only E_r profiles for a high plasma current (2.0 MA) and a low plasma current (1.0 MA) case are shown (Figs. 1 and 2 respectively). Figures 1 and 2 show the edge E_r profiles for two plasma discharges which are nearly identical in their plasma parameters and shape apart from the plasma current. Profiles of E_r are shown for L-mode conditions, early in the H-mode phase and later in time into the H-mode. The localization of the sheared region in E_r is well-defined with respect to the location of the separatrix, which is well resolved from the variation in the signal amplitudes of the CER chords spanning the separatrix. There is a decrease in the signal intensity of chords outside the separatrix and an increase in signal intensity inside the separatrix at the L-H transition.¹⁷ This allows us to determine the separatrix location in our data set independent of fits to magnetic probe data, although the separatrix location from both measurements typically agrees within the ± 0.5 cm error bars. Exact knowledge of the separatrix location is crucial because the E_r well is quite narrow. The depth of the E_r well in H-mode with respect to the L-mode value was the largest at the higher plasma currents and toroidal fields. This can be seen in Figs. 1 and 2 and in Table 1. The widths (FWHM) of the E_r wells are similar at about 1 cm, and a more critical determination of the E_r widths is limited to about ± 0.3 cm by the spatial resolution of the E_r measurement. No discernible structure in the E_r profile was observed during the L-mode phase of the discharge for any of the different plasma conditions.

The sharpest L-H transitions were observed in cases where the E_r profiles exhibited large minima. For example, in the plasma discharge corresponding to Fig. 1, the L-H transition (as observed on the divertor photodiode signal) occurred within 1 ms, whereas the photodiode signal for the plasma discharge corresponding to Fig. 2 indicated a gradual and dithering transition over a timescale of about 20 ms before the H-mode was firmly established. This seems to indicate that large values of E_r are correlated with faster L-H transitions and that once a critical value of E_r has been achieved the transition proceeds unhindered (or vice versa). This behavior does not prove causality. It only associates high E_r with faster L-H transitions. Nevertheless, the L-H transition for different plasma conditions occurs for an observed range of E_r values at the separatrix (Table 1) and the requirements for the change in E_r at the L-H transition may vary with different plasma conditions. The total input power (ohmic plus auxiliary heating) into the plasma discharge was maintained close to the threshold

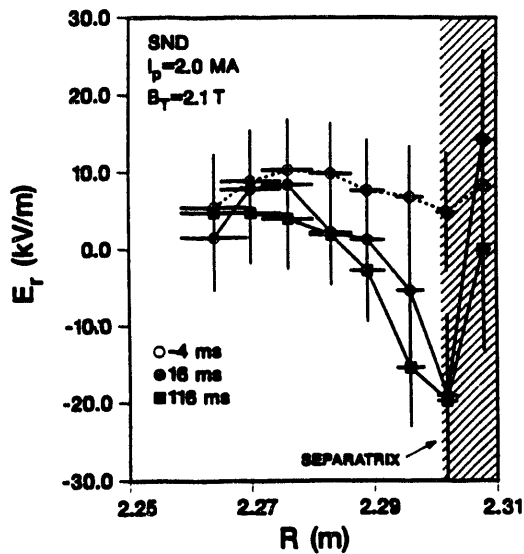


Fig. 1. The E_r profile for a plasma current of 2.0 MA. The shaded region is the uncertainty in the determination of the separatrix from fits to magnetic probe data. The times shown are with respect to the time of the L-H transition. The integration time of the measurement is 2.5 ms.

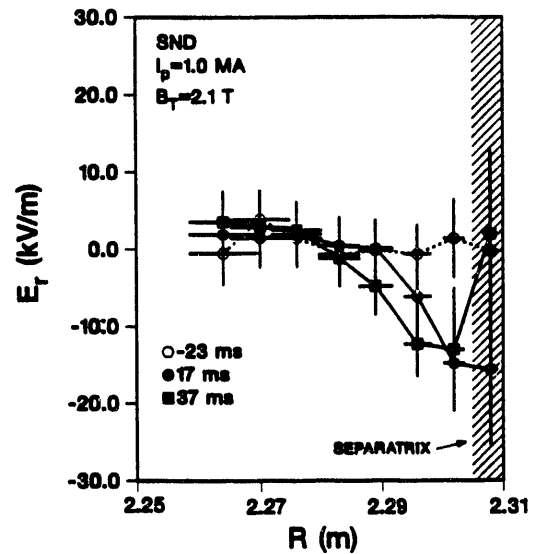


Fig. 2. The E_r profile for a plasma current of 1.0 MA. There is a movement of the separatrix of about 0.5 cm towards a lower major radius for the later H-mode time and does not represent a broadening of the E_r well. The integration time of the measurement was 2.5 ms.

TABLE 1
DESCRIPTIONS OF THE PLASMA CONDITIONS AND THE ASSOCIATED
WIDTHS AND DEPTHS OF THE E_r WELL AND THE VALUE OF $|\nabla E_r/B_T|$

All tabulated values are at the first available time after the L-H transition (i.e., within 20 ms after the transition). The value of $|\nabla E_r/B_T|$ is the largest determined value along the negative slope of the E_r well. The plasma conditions represent the departure of one parameter from the reference set of parameters. The reference set of parameters is: $I_p = 1.35$ MA; $B_T = 2.1$ T; \bar{n}_e (ohmic) = 4×10^{19} m⁻³; $\Delta Z_x = 14$ cm (for SND); outside gap = 6 cm; inside gap = 4 cm; triangularity = 0.85 (for DND).

Plasma Condition	E_r Width (FWHM) (cm)	E_{\min} - $E_{L\text{-mode}}$ (kV m ⁻¹)	$ \nabla E_r/B_T $ $\times 10^5$ Hz
SND reference condition SND; $I_p = 1.35$ MA; $B_T = 2.1$ T	1.1	-30	15.7
High plasma current SND; $I_p = 2.0$ MA; $B_T = 2.1$ T	1.2	-25	15.8
Low plasma current SND; $I_p = 1.0$ MA; $B_T = 2.1$ T	1.3	-16	6.2
Low toroidal field SND; $I_p = 1.35$ MA; $B_T = 1.5$ T	1.2	-14	6.7
Low plasma current and toroidal field SND; $I_p = 1.0$ MA, $B_T = 1.5$ T	1.2	-12	6.6
Low ohmic electron density SND; $I_p = 1.35$ MA; $B_T = 2.1$ T; n_e (ohmic) = 2×10^{19} m ⁻³	1.1	-13	5.7
Low divertor X-point location SND; $I_p = 1.35$ MA; $B_T = 2.1$ T; $\Delta Z_x = 0$ cm	1.0	-12	8.1
High divertor X-point location SND; $I_p = 1.35$ MA; $B_T = 2.1$ T; $\Delta Z_x = 24$ cm	1.2	-18	7.1
High plasma elongation SND; $I_p = 1.35$ MA; $B_T = 2.1$ T; $\kappa = 2.0$	1.2	-12	9.5
DND reference condition DND; $I_p = 1.35$ MA; $B_T = 2.1$ T	1.1	-25	9.5
Low toroidal field DND; $I_p = 1.35$ MA; $B_T = 1.3$ T	0.9	-15	15.4
Large inside gap DND; $I_p = 1.35$ MA; $B_T = 2.1$ T; $G_I = 8$ cm	0.8	-12	8.1

power required for the H-mode transition for times before, during and after the L-H transition so that any influence of excess heating power is reduced.¹⁸ The depth of the E_r well after the L-H transition appears to be lower at lower plasma current, lower toroidal field and lower ohmic electron density. Also, the power threshold for the H-mode for these cases is lower than for higher values of these plasma parameters in a single-null diverted discharge.¹⁹ Therefore, it seems as if the low power thresholds correspondingly have less deep E_r wells for these parameters. However, it is difficult to resolve as yet whether the depth of the E_r well is a stronger function of the input power or of the plasma parameters. The contributions to the total radial electric field from the diamagnetic and rotational terms of the force balance equation were examined. For *all* cases, the greatest contribution to E_r at the L-H transitions resulted from the change in the impurity ion poloidal rotation. The influence of the impurity ion pressure gradient term becomes appreciable 10's of milliseconds later in time into the H-mode. However, it has been shown^{14,15} that the main ion poloidal rotation 3.5 ms after the L-H transition is in the ion diamagnetic direction and opposite to the impurity ion poloidal rotation, as pointed out by neoclassical theory.²⁰ By this time, the main ion pressure gradient term is the dominant, negative term in the determination of E_r and remains so thereafter through the H-mode. No conclusions can be made discriminating between the $\partial P_I/\partial r$ and $V \times B$ terms for the impurity ions and main ions in this study, apart from the fact that for all the plasma parameters studied, the poloidal rotation for the impurity ions is consistently in the electron diamagnetic direction and is the important term at the time of the L-H transition. Even though there is no clear disagreement with the observed E_r widths and Shaing's modified theory²¹ which includes the influence of the shear in E_r on the banana orbit widths, the dominance of the main ion pressure gradient milliseconds after the L-H transition^{14,15} would imply that the observed E_r structures reflect the behavior of the main ion pressure gradient profiles⁹ for the various plasma parameters.

The E_r shear suppression theory of Biglari, et al.⁷ predicts that shear in E_r can nonlinearly stabilize a range of flute-like turbulent modes with the criterion for effective suppression being $|\nabla E_r/B_T| \geq (\Delta\omega_t/k_\theta\Delta r_t)$ where B_T is the toroidal field, $\Delta\omega_t$ is the turbulent decorrelation frequency, Δr_t is the radial correlation length, and k_θ is the mean poloidal wave number of the turbulence. The values of $\Delta\omega_t$ and Δr_t are in the absence of the electric field shear. Using typical values of $2\pi \times 40$ kHz for $\Delta\omega_t$ (from reflectometry measurements), 0.7 cm for the radial correlation length Δr_t and 1 cm⁻¹ for k_θ , the RHS of the above criterion is equivalent to 3.6×10^5 Hz. The E_r profiles at the L-H transition for the various plasma parameters studied were analyzed for the value of the $|\nabla E_r/B_T|$. These values are shown in Table 1 and represent the largest shear in E_r inside the separatrix. Note that the values of $|\nabla E_r/B_T|$ are underestimates since the spatial resolution of the E_r measurements leads to averaged

determinations of E_r over a finite spatial region. Nevertheless, Table 1 clearly shows that the criterion of Biglari et al., for E_r shear stabilization of turbulence is satisfied by between a factor of 2–5 for $k\theta \geq 1 \text{ cm}^{-1}$ for all the plasma conditions investigated.

The greatest changes in the E_r profile after the L–H transition were observed for the case of the low ohmic target electron density discharge. The E_r profiles for this discharge are shown in Fig. 3. There is an increase in the depth of the E_r well and a broadening of the well with time into the H–mode at constant input power. The main reason for the broadening is the increasing spatial extent of the region with the high pressure gradient, which is much more important later in the H–mode for the low density discharge than in the other cases. This is qualitatively in agreement with the theory of Hinton and Staebler, which links the mean free paths of incoming neutrals with the width of the region of high pressure gradient. The deeper penetration of neutrals at lower electron densities would then favor a broadening of the E_r profile.

In summary, there is no clear variation in the shape or width of the E_r well at the L–H transition with any of the different plasma parameters investigated. The value of E_r is negative just inside the LCFS for all cases. There is a variation in the depth of the E_r well for different conditions and the largest broadening of the E_r width later into the H–mode is observed in the case with a low ohmic electron density. The criterion of Biglari et al., for the suppression of turbulence by sheared $E \times B$ flow is satisfied for all the cases.

¹K. H. Burrell, et al., Phys. Fluids B 2, 1405 (1990).

²R. J. Groebner, et al., *Plasma Physics and Controlled Nuclear Fusion Research*, 1990 (International Atomic Energy Agency, Vienna, 1991), Vol. 1, p. 453.

³E. J. Doyle, et al., Phys. Fluids B 3, 2300 (1991).

⁴P. Gohil, et al., in *Proceedings of the 18th European Conference on Controlled Fusion and Plasma Physics*, Berlin, 1991 (European Physical Society, Petit-Lancy, Switzerland, 1991), Vol. 15C, p. 289.

⁵K. Ida, et al., Phys. Fluids B 4, 2552 (1992).

⁶K. H. Burrell, et al., Plasma Phys. Controlled Fusion 34, 1859 (1992).

⁷H. Biglari, et al., Phys. Fluids B 2, 1 (1990).

⁸K. C. Shaing, et al., Phys. Fluids B 2, 1492 (1990).

⁹F. L. Hinton et al., Phys. Fluids. B 5, 1281 (1993).

¹⁰A. B. Hassam, et al., Phys. Rev. Lett. 66, 309 (1991).

¹¹P. H. Diamond, et al., Phys. Rev. Lett. 72, 2565 (1994).

¹²B. A. Carreras, et al., Phys. Fluids B 5, 1491 (1993).

¹³K. C. Shaing, Phys. Plasmas 1, 219 (1994)

¹⁴J. Kim, et al., Phys. Rev. Lett. 72, 2199 (1994).

¹⁵K. H. Burrell, et al., Phys. Plasmas 1, 1536 (1994).

¹⁶P. Gohil, et al., in *Proceedings of the 14th IEEE/NPSS Symposium on Fusion Technology* (Institute of Electrical and Electronics Engineers, Princeton, NJ, 1992), Vol. II p. 1199

¹⁷P. Gohil, et al., GA-A 21265 to be published Nuc. Fus.

¹⁸R. J. Groebner, et al., in *Proceedings of the 19th EPS Conf. Contr. Fusion & Plasma Phys.* (Innsbruck, 1992)

¹⁹T. N. Carlstrom, et al., GA-A21541, to be published in Plas. Physics and Contr. Fusion.

²⁰Y. B. Kim, et al., Phys. Fluids B 3, 2050 (1991).

²¹C. Shaing, Phys. Fluids B 4, 171 (1992).

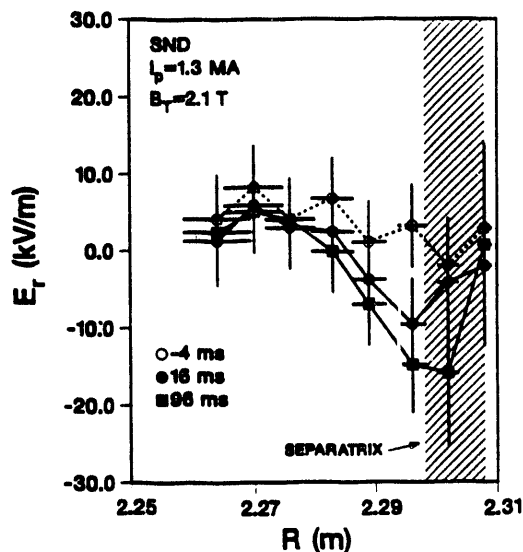


Fig. 3. Profiles of E_r at various times for a plasma discharge with low ohmic electron density, \bar{n}_e , of $2 \times 10^{19} \text{ cm}^{-3}$. The times shown are with respect to the time of the L–H transition. The integration time for each profile is 2.5 ms.

DATE

FILMED

9/29/94

END

